J Mater Sci (2006) 41:6526–6546
DOI 10.1007/s10853-006-0196-3

Failure processes in composite materials: getting physical

P. W. R. Beaumont · R. A. Dimant · H. R. Shercliff

Published online: 8 August 2006

Abstract This paper describes crack growth processes in carbon fibre and glass fibre-epoxy laminates under stress and quantifies by physical modelling the accumulation of damage with load cycling. Cracking mechanisms are observed directly and identified by in-situ dynamic scanning electron microscopy. Armed with this information, particular attention is given to the differences between these cracking processes and the way they interact, their growth-rate, and their effect on the damage-state of the structure with variations in laminate geometry, with changes in magnitude of applied stress, and with fatigue cycles. Particular attention is given to the internal damage state variable approach to physical modelling.

Predictive modelling of the behaviour of composite materials

For half a century, factors that influence the limits of performance of engineering composite materials and the capability of large structures and components to sustain high stresses without failure, have been the subject of many analytical and theoretical investigations, validated by observations and precise measurement of property data. Yet despite this acquisition of vast collections of information and compelling evidence, and an experienced designer's intuition based on ''feel'', ''know-how'' or ''folklore''—a *phenomenology*—our ability to fully understand composite material behaviour remains restricted. Oversight in design across orders of magnitude of size of structure has led to undesirable matrix-dominated load paths. In composite structures under load, this has resulted in the cumulative evolution of a complexity of inter-acting small defects. This is material failing on the nanometre or micron size scale, and we notice its consequences at the component level. There still remains the difficulty in connecting results at the different scale levels. Of particular interest is how damage transfers from a lower scale to a higher scale [1–3]. Moreover, when mechanisms of cracking interact, superposition becomes important. And if those interactions are non-linear, simple constitutive laws break down.

Our comprehension of structural changes in composite materials, however, which take place continuously and cumulatively, is lacking in detail. More often than not, these simultaneously acting microscopic (or atomistic) processes are simply not known. Consequently, current design codes for composite material structures in critical loading situations do not take creep, fatigue and environmental-induced mechanisms into account. To predict a result, say lifetime or a stress response by a numerical method, there must be a self-evident truth that the mechanism regime in which the component is operating must be known. In other words, the important design issues must all be embedded in the same model of material and component behaviour that must also include the dominant mechanism(s) of structural change over orders of magnitude of size. Furthermore, what makes for a successful and safe application varies from one material system to the next. Their diversity of failure characteristics stems from the differences between fibre-matrix systems and the nature of

P. W. R. Beaumont (✉) · R. A. Dimant · H. R. Shercliff
Engineering Department, Cambridge University , Trumpington Street, Cambridge CB2 1PZ, England
e-mail: pwb1000@hermes.cam.ac.uk

bonding between the constituent phases. It is not surprising then, that identifying the dominant process(es), meaning the one (or more) that has the most influence on the material's or component's limit of performance is not straightforward and sometimes the problem contains several sub-problems. To model each sub-problem separately and to combine the results later, if that is possible, requires that phenomenology—experience, comprehensive collections of data, etc—knowledge based on intelligent observations.

Also required, is the determination of their dependencies on stress, on temperature and environment, and time. And if there is no such phenomenology, then it will be necessary to generate one by conducting experiments. In other words, the constitutive equations of continuum design remain firmly based on direct experimental evidence. Difficulty arises, of course, when experimental conditions become so stringent, that even more properties are involved in the design process at all levels of size. What are needed, of course, are constitutive equations for design that encapsulate all of those intrinsic and extrinsic variables. Obviously, the experimental programme from which these constitutive laws are to be devised becomes formidable. And if that is not enough, spatial variation appears when stress and temperature or other field variables are non-uniform. While simple geometries can be treated analytically, using, for example, the modelling tools of fracture mechanics, more complex geometries require discrete methods. The finite element method of modelling is an example. Internal material state variable formulations for constitutive laws are embedded in the finite element computations to give an accurate description of spatially varying behaviour.

Understanding the significance of damage growth mechanisms

Oversights in composite material design have led to matrix-dominated load paths resulting in the nucleation of a multiplicity of cracks and the accumulation of damage in the component under stress. Consider, for example, the fibre strengthening of a cross-plied polymeric matrix laminate: typical damage consists of several forms of matrix-dominated cracking processes, such as cracking of the transverse (90^o) ply, and de-lamination cracking between the transverse and longitudinal (0^o) ply. Furthermore, the intensification of localised stress at the tip of a transverse ply matrix crack could be sufficiently large to initiate the breakage of neighbouring fibres in the adjacent load-bearing (0^o) ply. In many (perhaps all) composite material systems, such damage would lead to catastrophic fracture of the component.

Basically, what is required in the design of a damage-tolerant material is the presence of a *microscopically weak* structure built into a *macroscopically strong* solid that ensures any crack present becomes innocuous. An example is where a fibre-matrix interface fails by de-cohesion and, in so doing, blunts the tip of a small propagating matrix crack whilst the fibres bridging that crack remain intact. This central problem of crack propagation resistance on planes normal to the fibre reinforcement axis has been confronted [4–8]. Whilst available models have focused on the question of fracture processes (*mode I* tensile) behind the matrix crack front perpendicular to fibres, those fracture processes, which occur in the crack tip field, (the damage process zone), have received less attention. The question of the mechanisms of *mixed-modes I and II*, splitting and de-lamination cracking, and matrix cracking, which spreads throughout the composite over time, requires resolution. Furthermore, the role of fibre fracture in the fatigue process, particularly in hostile environment, is only partially understood [9–13].

Physical model development based on actual failure mechanisms

As with most (perhaps all) materials, the weakening of the composite brought about by the accumulation of structural changes over time begins, more often than not, with localised cracking at points of load concentration. Examples of load concentrations in a laminate include: a ply drop, a hole or notch or other discontinuity such as a cut-out, a bolted or adhesive joint, an abrupt change in contour, a manufacturing defect such as fibre ends, or a free-edge. At the micro-structural level, randomly dispersed micron-sized cracks, including broken fibres, also act as stress concentrators. In this respect, we shall consider the fatigue behaviour of a family of cross-ply $(0_i/90_j)_{ns}$ laminates where the intensified stress at the tip of a microscopic-sized transverse ply (matrix) crack induces de-lamination cracking at the interface between the off-axis ply and the longitudinal ply, and the start of a sequence of fractures of the load-bearing fibres that eventually leads to catastrophic failure of the component.

Ideally, the route to take begins with the identification of those dominant (meaning most damaging) failure mechanism(s), which then leads to the proposal of a sound *physical* or *mechanism-based model*, one that captures the essential physics of the material (or engineering) problem of fracture, whether it is induced by simple monotonic tensile loading or by repeated (meaning cyclic) loading. The development of such a model relies strongly on the existence of a concise description of a body of fatigue or

fracture stress or modulus (stiffness) data that relates directly, in one way or another, to the particular mechanism(s) of cracking affecting the overall failure process. In other words, the fatigue variables like maximum stress, stress range or stress amplitude, loading frequency and pattern, numbers of load cycles, temperature, environment, internal material damage-state, must all be embedded in the same physical model that also includes the principal mechanism(s) of failure.

Identifying the major failure mechanisms, meaning those ones that have the most influence on a material's strength or on a component's performance, may sound straightforward but sometimes the problem contains several sub-problems. For example, in the accumulation of fatigue damage in a cross-ply composite material, at least three matrix-dominated cracking mechanisms are involved and they do interact. The propagation of a matrix crack in a transverse (90^o) ply will interact with the formation of a de-lamination crack between that ply and, consequently, influences the load in the adjacent (0^o) ply in the complete damage zone [14, 15]. Snapping of those primary strengthening fibres in turn over prolonged periods of time will eventually trigger a series of complex events that result in the catastrophic fracture of the material.

To model each sub-problem (event) separately and to combine the results later, if that is possible, requires a *phenomenology*—experience, collections of data of crack growth-rates and property changes, a quantitative knowledge of transverse ply cracking, of de-lamination cracking, of fibre fracture, and so forth. Also required, is the determination of their dependencies on stress [16–24], time (or load cycles) [16–19, 25–29], temperature [30–33], and on environment [12, 13]. If there is no such phenomenology, then it will be necessary to generate one by conducting experiments. The material variables, which are inputs to the model, will include laminate lay-up geometry or fibre orientation, ply thickness and number of plies; and the boundary conditions will include, stress-state, number of load cycles (time), cyclic frequency, temperature, and environment. Ideally, we require, by direct observation, if possible, the identification, classification and assessment of the importance of these mechanisms of cracking under those conditions that the component will experience in service.

Damage state in a laminate under tensile stress

Structure change (by damage accumulation) is exactly that: the structure or damage within the material evolves with time (or number of load cycles) in service. When the composite is loaded to a critical stress, internal cracks form and accumulate within it. This ''damage'' spreads throughout the material and weakens it, and reduces the material's stiffness, which in turn increases the rate at which further damage accumulates: there is positive feedback.

A response equation can be derived which describes (say) the relationship of current modulus E, (a measure of the effect of damage on stiffness of the laminate), to the cyclic stress range $\Delta\sigma$, and the current value of an internal state variable, which we shall call D (for damage). (This is often the area fraction of cracks that evolves during fatigue [16–19]). We call these internal variables ''damage'' because they describe a change in the state of a material, brought about by fatigue in this instance. The state variable D evolves with the progressive nature of fatigue damage and describes the current state of the composite's structure. It is important to realise that the dominant mechanism(s) of cracking can change as the total failure process progresses, leading to a catastrophic finale.

The onset of these changes in dominance of failure mode depends on the independent variable stress range, $\Delta\sigma$, (with maximum stress, $\sigma_{\max}$, frequency, ν, and temperature constant). With only one such variable, a fairly complete characterisation is practicable. But this does not cater for time-varying stress $\Delta\sigma$ (t) and fluctuating temperature $\Delta T(t)$, or for the effect of changes in stress-state on the fatigue cracking processes. If we try to include them in a model for current modulus, we find we are dealing with eight or more independent variables: temperature T, stress σ, the frequency (ν_σ, ν_T) and amplitude (ΔT, $\Delta\sigma$), the ratios λ of stress invariants, and so forth:

$$E = f(\sigma, \lambda, T, t, \Delta\sigma, \Delta T, \nu_\sigma, \nu_T, \text{material properties, laminate geometry}) \quad (1)$$

Moreover, with the added number of variables included in the material properties and laminate geometry, we get 16 or more.

Nevertheless, it is still possible to set up an experimental program to characterize the influence of each of these variables on fatigue; that is the direction in which research has traditionally followed [1–3]. But the scope of the test program would be immense. More often than not, it can be further complicated because of the numerous and interacting mechanisms of fracture and fatigue involved. Likewise, characterisation of material behaviour over one range of temperature (for instance) cannot safely be extrapolated into another; a new characterisation is needed. The method of extended empiricism just breaks down under the unmanageable load of variables.

Successful models for composite fatigue behaviour have one thing in common; they contain the internal state variable D, the parameter that characterizes the current mechanical state of the material. But instead of trying to characterize a material property, for example, modulus, E,

as a function of the independent variables, we now seek to fit data to a coupled set of differential equations [16–19], one for the modulus E', and one, two (or more) depending on the number of damaging mechanisms for damage evolution, D_1' and D_2' and so on.

For the rate of change of modulus, E, and damage, D, we have:

$$E' = f_1(\sigma, \lambda, T, D_1, D_2, \text{material properties, laminate geometry}) \quad (2a)$$

$$D_1' = g_1(\sigma, \lambda, T, D_1, D_2, \text{material properties}) \quad (2b)$$

$$D_2' = g_2(\sigma, \lambda, T, D_1, D_2, \text{material properties}) \quad (2c)$$

D_1 describes the damage due to one mechanism and D_2 describes a different damaging mechanism that when combined with the former leads to composite failure. E', D_1' and D_2' are their *rates of change* with time (or number of cycles); f_1, g_1, g_2 are simple functions that can be determined by experiment. (Fig. 1)

Now there are three independent variables (σ, T, and stress-state, λ). These equations can be integrated to track out the evolution of modulus and damage, and ultimately to predict fracture of the material or design (safe) life of a component. The modulus-time (cycles) response is found by integrating the equations as a coupled set, starting with $E = E_o$ (the undamaged modulus) and $D = 0$ (no damage unless damage D_i has been introduced during fabrication, or by earlier history). Cyclic loading causes the damage to increase from D_i to D_f at which point the weakened composite undergoes catastrophic failure, i.e., the applied (working) stress exceeds the (reduced) strength of the material. Step through the time (cycles) history, calculating the increments, and thus the current values, of E and D, and using these to calculate their change in the next step to construct Fig. 2 below [16–19]. Equation (2) can now be adopted as the constitutive equation for fatigue, and empirical methods can be used to determine the functions f_1, g_1, g_2. So, empiricism still has a part to play.

In Fig. 2, we see that with increasing numbers of load cycles at low cyclic stress, $\Delta\sigma_1$ (so called high cycle fatigue), the modulus falls gently with the accumulation of slowly propagating transverse ply cracks. As stress amplitude increases, $\Delta\sigma_2$ a change in slope at a lower number of cycles designates the onset and domination of

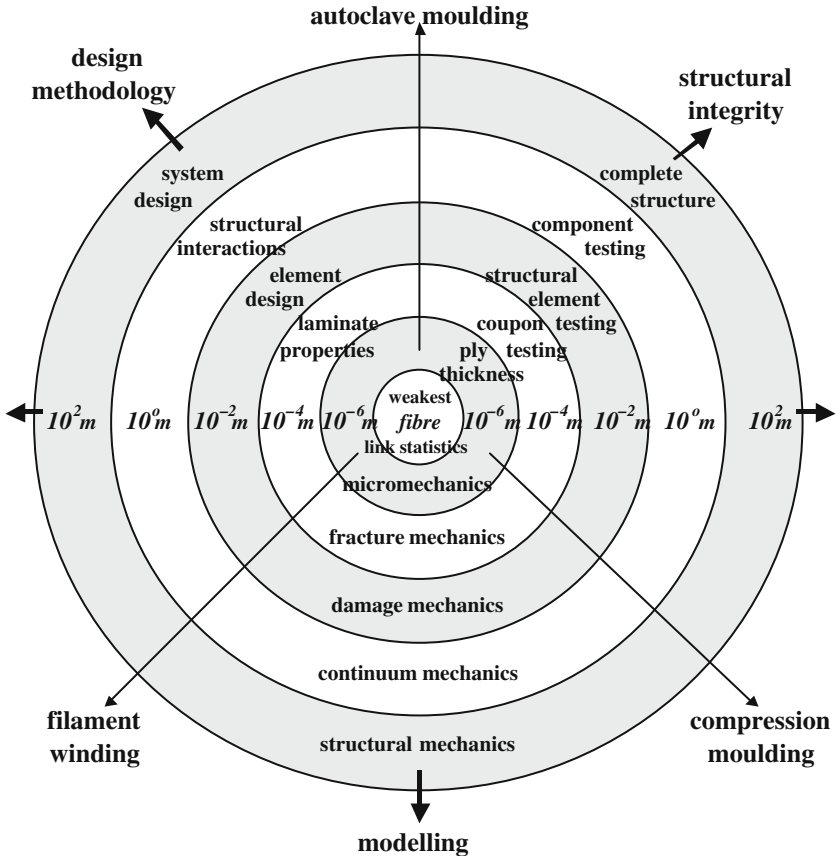

Fig. 1 Hierarchy of structural scales ranging from the micron to the metre (and greater) level of size, from the single fibre to the fully assembled structure, and discrete methods of analysis in design ranging from micro-mechanics to the higher structural levels of modelling

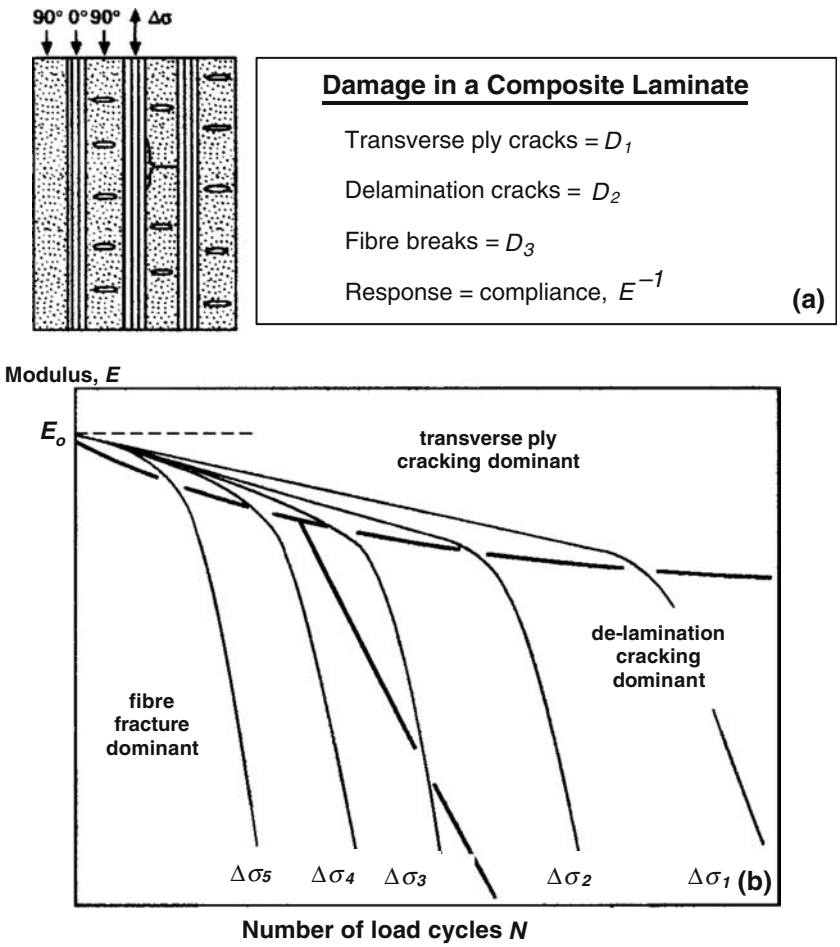

Fig. 2 (**a**) A model of the composite laminate subjected to repeated load cycling $\Delta\sigma_1$, $\Delta\sigma_2$, $\Delta\sigma_3$ etc, with transverse ply cracks, de-laminations, and fibre fractures—state variables D_1, D_2, D_3 measure the extent of these damaging mechanisms. (**b**) Response E, with the dominant failure mechanisms identified; a fatigue failure map

de-lamination cracking. And if the stress amplitude increases even further, (greater than $\Delta\sigma_3$) (now called low cycle fatigue), the critical mechanism becomes one dominated by fibre fracture. Thus, the various modes of failure spread throughout the composite until either the net section stress, (there is a loss of section caused by the damage), exceeds the tensile strength, or a crack of critical size has evolved, by the linking of these microscopic-sized cracks. Having attained a critical size, this crack (formed from this complexity of inter-acting cracks) then propagates catastrophically across the section accompanied by a cascade of breaking fibres [5].

The path to follow for successful modelling is one that leads to design equations having predictive powers capable of producing the fatigue failure map shown in Fig. 2. It takes us to an understanding of the underlying microscopic cracking mechanisms responsible for changes in structure and material property, which is followed by the development from first principles of a physical model for each stage of the total fracture process. Success has been limited: a problem arises because of the numerous microscopic parameters that define the structure and that can only be determined by microscopic means and observation, and this is difficult to overcome in practice.

Internal structure and damage characterisation

The identification of failure mechanisms is best established by experimental means: for example, by in-situ dynamic scanning electron microscopy (SEM), which provides a powerful means of observing mechanisms in action. For internal crack formations, use can be made of X-rays to observe them. Alternatively, but less satisfactorily, these mechanisms may be inferred by indirect means: by monitoring changes in modulus or damping capacity (mechanical hysteresis) or Poisson's ratio, by measuring changes in electrical conductivity, or light scattering, or X-ray absorption, or ultrasonic attenuation, or by acoustic emission detection. Actual failure mechanisms can also be inferred by carrying out post-mortem examination of fractured or damaged materials using conventional SEM.

But it is most important to remember, however, that it is dangerous to assume a mechanism without real evidence of

its actual operation. Furthermore, it is unwise to take for granted, (unless it has been proven without a shadow of doubt), that an identified mechanism is the only one or that it is the dominant one amongst others. Dominant in this sense means the most influential mechanism in the overall failure process, by having the major effect on weakening the material's mechanical properties or limiting the component's performance in service. Primarily, we require the resolution of mixed-mode failure processes throughout the entire laminate, of matrix cracking, of splitting and of de-lamination cracking. A thorough understanding of these failure modes coupled to fibre fracture is important. A complete picture enables the formulation from first principles of a physical model that is capable of predicting the stiffness (modulus), the fracture stress and post-fatigue behaviour of the final component.

Identifying mechanisms of cracking by in-situ dynamic SEM

Many, (perhaps all), composite systems under load crack throughout their life time by a number of different failure mechanisms, and they can be identified directly by in-situ dynamic scanning electron microscopy (SEM) and optical microscopy. Figure 3 shows optical photomicrographs of a damaged cross-ply $(0°_i/90°_j)_{ns}$ glass fibre-epoxy laminate by monotonic (or cyclic) tensile loading, where failure, first and foremost, is by the evolution of a multiplicity of cracks in the matrix of each transverse (90°) ply. These closely spaced cracks lie roughly parallel to one another, and in a plane that is perpendicular to the direction of applied stress; and they span the thickness and width of every transverse ply. More often than not, depending on transverse ply thickness, a microscopic-sized de-lamination crack, (sometimes called an inter-laminar crack), nucleates by de-cohesive failure of the (0°/90°) interface, in front of the tip of an advancing matrix crack.

This has been identified by in-situ SEM (Fig. 4). In the SEM photomicrographs of Fig. 4, the laminate is loaded in fatigue with a maximum tensile stress close to the laminate fracture stress and we observe the transverse ply crack spacing to be about twice the ply thickness. The de-lamination crack, which initiates at the matrix crack tip, extends stably by *mode II* (shear) deformation in the epoxy resin and by interfacial de-cohesion (Fig. 5). Inter-section of the matrix crack tip with the de-lamination crack surface seems inevitable. Furthermore, some fibres may fracture within the adjacent (0°) ply at sites close to the plane of the matrix crack (Fig. 6a). They do so because the local intensification of tensile stress in the vicinity of the matrix crack tip exceeds the fibre strength. From Fig. 6(b), we infer that the transverse ply crack extends into the longitudinal (0°) ply leaving fibres intact in its wake, before they finally snap. More fibre breaks in the vicinity of a transverse ply crack can be seen in Fig. 7.

We believe there are two possible alternative reactions to the localised stress field surrounding the matrix crack tip: either, the de-lamination crack forms, blunting the matrix crack tip and thereby reducing the tip stress intensity, or the interfacial bond between the off-axis (90°) ply and (0°) ply remains intact and there is no de-lamination. If the latter prevails, which, as we shall see later, is the case for laminates containing ''thin'' transverse plies, (i.e., where $j \leq 2$, (as in $(90°_j)$), then the magnification of local tensile stress can initiate the breakage of fibres in the adjacent load bearing (0°) ply, on or close to the matrix crack plane (Fig. 7). As a consequence, the stiffness (modulus) of the laminate decreases, and the material ''softens''; it becomes more compliant. This necessarily implies that thickness of the transverse ply is a major factor in determining the mechanisms of cracking, the ''reduced'' modulus, and post-fatigue strength of the damaged laminate. In our in-situ dynamic SEM monotonic and cyclic loading tests, we observed and measured the transverse ply (matrix) crack spacing and the de-lamination crack length (at the matrix crack tip). This information provides the failure mechanism(s) input to our physical model, which we develop next.

Physical modelling of coupled mechanisms of damage accumulation

The physical picture is one of damage accumulation by the coupling of transverse ply (matrix) cracking and de-lamination cracking at the matrix crack tip. Alternatively, (or simultaneously), this leads to fibres (of the longitudinal ply) snapping in the vicinity of these matrix crack tips. Figure 8 shows a much-simplified representation, and for the time being, the model does not include fibre fracture. It is important to understand the interaction (coupling) between these two failure processes and their influence on fibre fracture and the resulting (damaged) mechanical properties of the composite.

In this model or artist's impression of the real thing, a matrix crack is shown inter-secting a de-lamination crack (circled). Spacing between one pair of adjacent matrix cracks is depicted $2s$; for the evolution of this mechanism only, we would define our ''damage'' parameter simply as $D = (2s)^{-1}$. In the sketch, the de-lamination crack length is denoted ℓ_d. The thickness of an individual transverse (90^o) ply is d; and b is the thickness of an individual (outside) longitudinal (0^o) ply. The width of the specimen, not shown in this simple edge view, is denoted w.

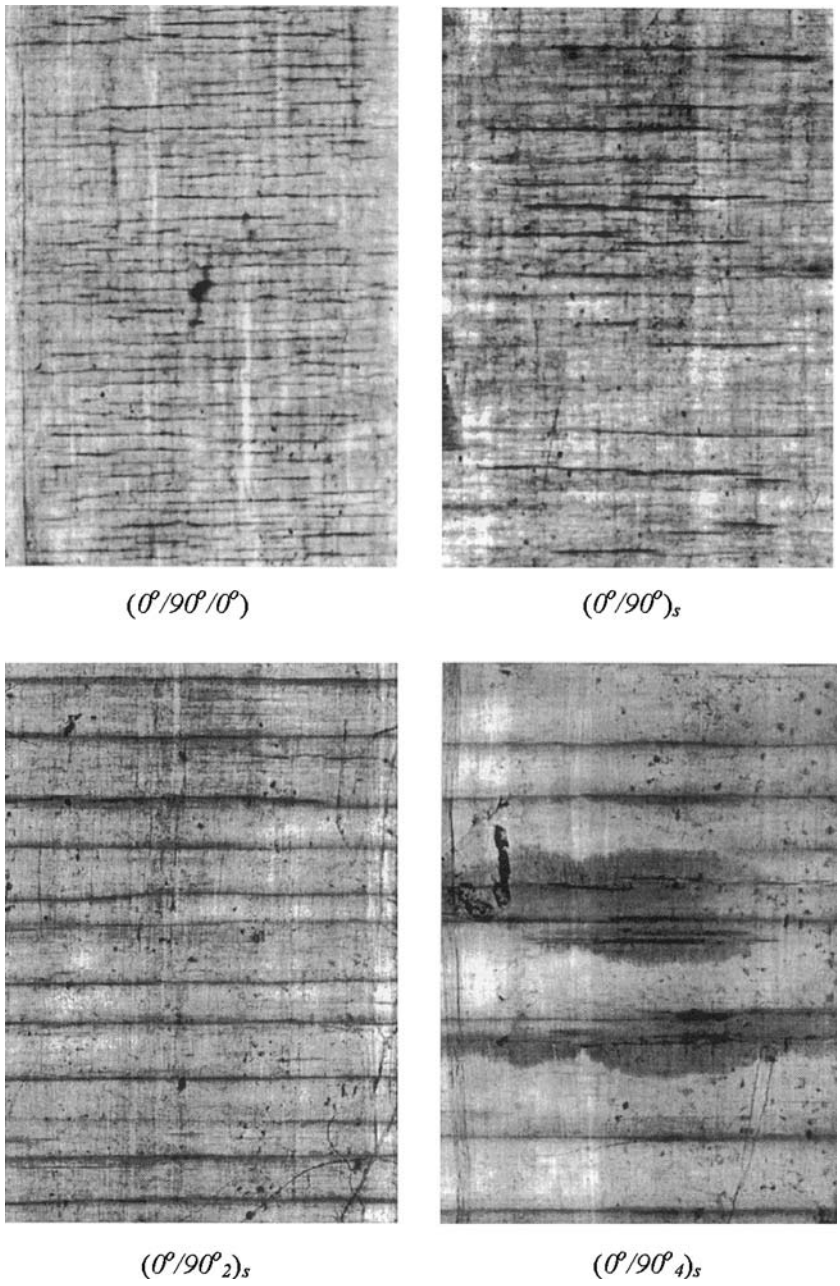

Fig. 3 Transverse ply (matrix) crack spacing in cross-ply glass fibre-epoxy laminates observed by in-situ SEM. These specimens were fatigued at 600 MPa for 10,000 cycles (6 mm section shown)

This model of a ''damage zone'' consists of two parts: that portion of material that is cracked, which we have designated (*a*) (circled in Fig. 8), and that portion designated (*b*) where the (0^o/90^o) interface remains intact between the tips of two approaching de-lamination cracks. In effect, damage accumulates as the matrix crack spacing gets smaller, while the de-lamination crack grows longer. Consequently, the distribution of applied load between portion (*a*) and portion (*b*) of the laminate is continuously re-adjusting. It is this re-adjustment of load between adjacent (0^o) and (90^o) plies with damage accumulation that either brings about the fracture of the load carrying (0^o) fibres, or not. Final (catastrophic) fracture of the material depends ultimately on this balance.

Estimating the modulus (or stiffness) of the laminate

To begin with, assume matrix cracking only; ignore for the time being the possibility of microscopic de-lamination cracking and fibre fracture. The localised crack tip tensile stress in the longitudinal (0^o) ply and the transverse (90^o) ply (containing the matrix cracks spaced $2s$ apart), with distance x from the crack plane, can be estimated using Eqs. (3) and (4), respectively, which have been developed from a shear lag model and used extensively (16–19):

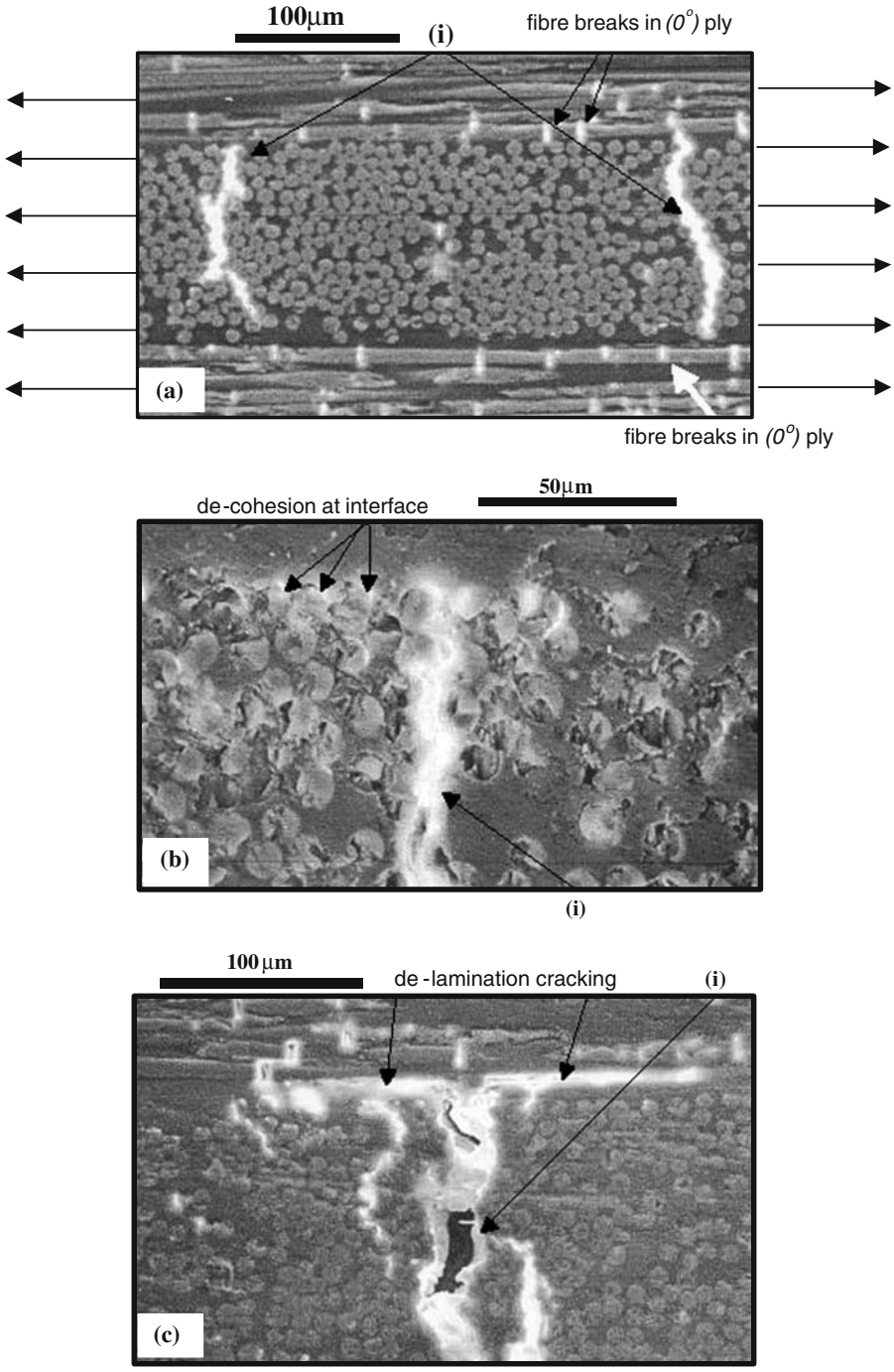

Fig. 4 Adjacent transverse ply cracks (i) in (0/90/0) glass fibre-epoxy close to failure. Crack spacing is close to twice the ply thickness in (**a**)

$$\sigma_1 = \left[\frac{E_1}{E_2} + \left(\frac{dE_2}{bE_o}\right)\frac{\cosh(\lambda x)}{\cosh(\lambda s)}\right]\sigma_a \tag{3}$$

$$\sigma_2 = \frac{E_2}{E_o}\left[1 - \frac{\cosh(\lambda x)}{\cosh(\lambda s)}\right]\sigma_a \tag{4}$$

E_1 and E_2 are tensile moduli of the longitudinal and transverse plies, respectively; E_o is the (un-damaged) laminate modulus, (the situation where there are no matrix cracks); and σ_a is the remotely applied tensile stress on the laminate. (The value of the coefficient, λ, lies somewhere between 1 and 3, depending upon whether the variation in

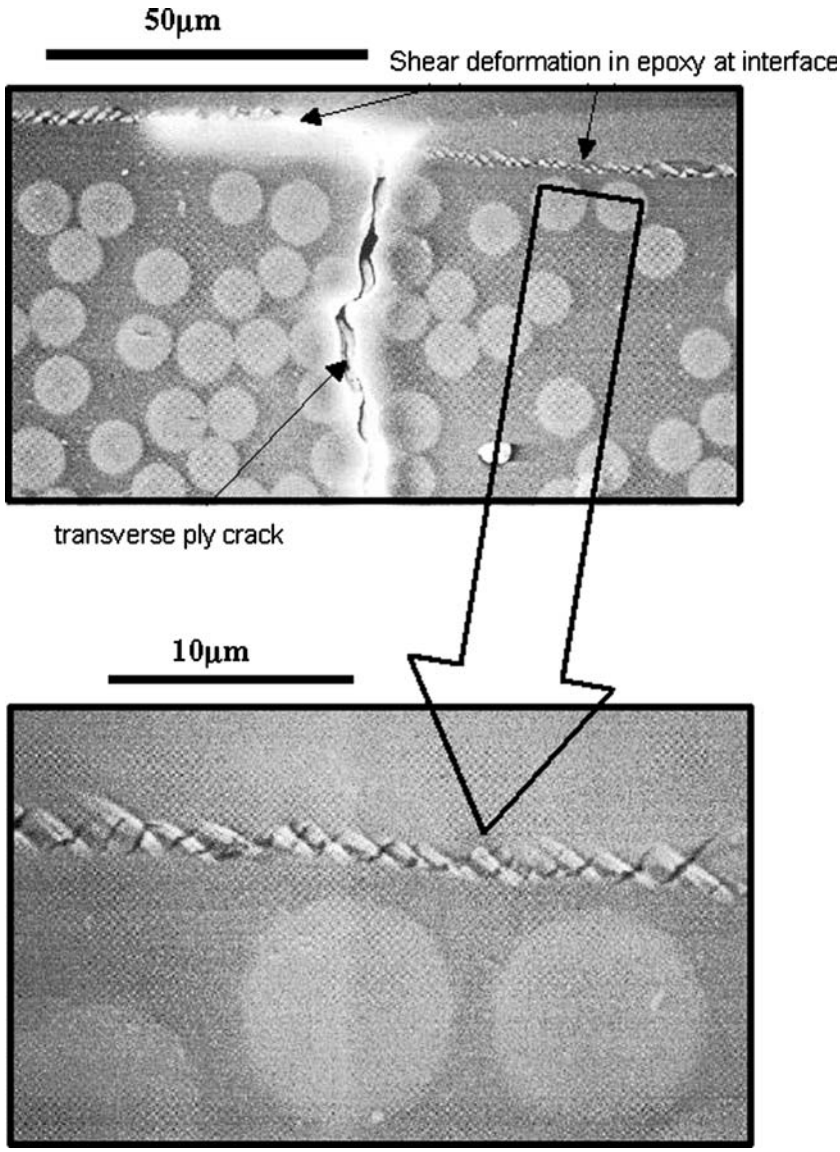

Fig. 5 Intersection of a transverse ply crack with the longitudinal ply in a $(0/90_4)_s$ glass fibre-epoxy after 10,000 load cycles at 600 MPa showing plastic (45^o) shear deformation bands in the epoxy close to the (0/90) interface

stress with distance, x, obeys a linear or parabolic shear displacement law. Either way, it affects the final result little).

For small elastic strain in the longitudinal ply, and determining the mean stress in the longitudinal ply, (obtained by integrating Eq. (3) with respect to distance x), we obtain the following expression for reduced modulus, E_c, of a matrix-cracked laminate [16–19]:

$$\left[\frac{E_c}{E_0}\right] = \frac{1}{\left[1 + \left(\frac{dE_2}{bE_0}\right)\frac{\tanh(\lambda s)}{\lambda s}\right]} \tag{5}$$

It is convenient to make Eq. (5) dimensionless by normalising E_c with respect to the un-damaged modulus E_o. Roughly speaking, the modulus of an un-damaged laminate, (meaning there are no matrix cracks unless prior damage was done), can be determined using a simple rule of mixtures:

$$E_0 = \left[\frac{bE_1 + dE_2}{b + d}\right] \tag{6}$$

At this point, we can now extend this model to include microscopic de-lamination cracking at the matrix crack tip as follows [14]. Begin with the assumption that the reduced (or damage) modulus, E_c, of that de-laminated portion of laminate, (previously designated *(a)* in Fig. 8), depends essentially on the modulus of the longitudinal (0^o) ply only:

$$\left[\frac{E_c}{E_0}\right]_a = \left[\frac{bE_1}{bE_1 + dE_2}\right] \tag{7}$$

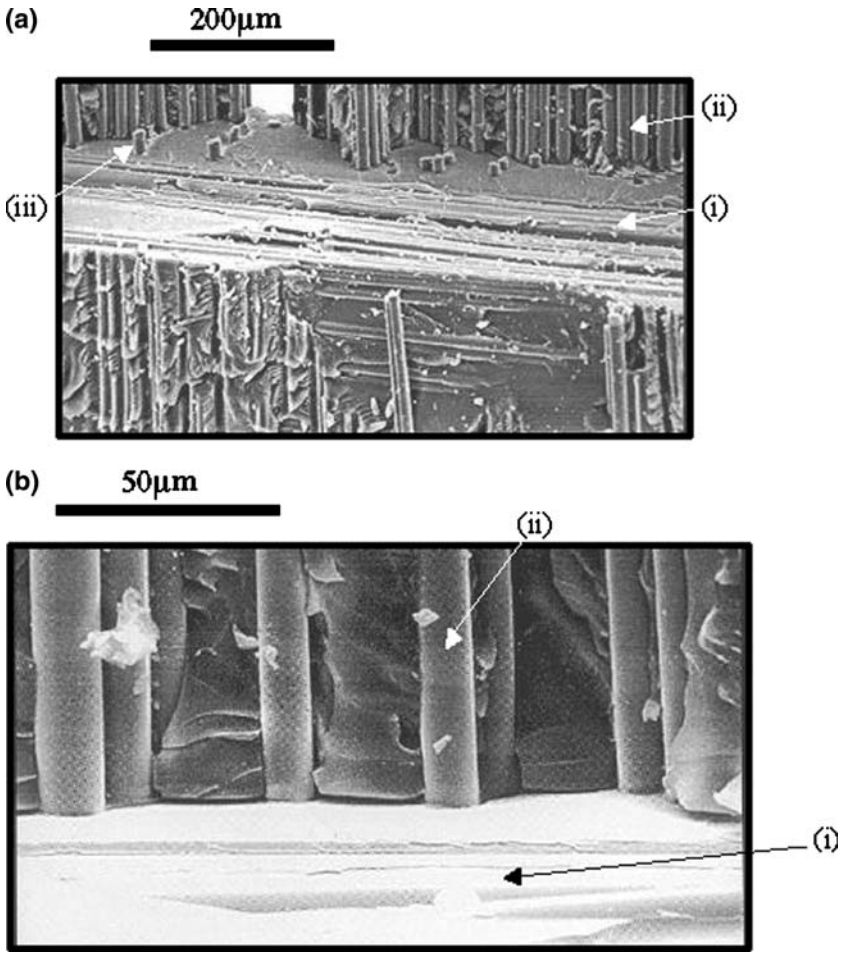

Fig. 6 (**a**) Fracture surface of a transverse ply crack (i) intersecting with the adjacent longitudinal ply that has de-laminated (ii). Broken (0^o) fibres can be seen in the proximity of the plane of the transverse ply crack tip (iii). This is a $(0/90)_s$ glass fibre-epoxy laminate fatigue loaded. (**b**) Penetrating transverse ply crack (i) into the adjacent longitudinal ply that has de-laminated (ii). This is a $(0/90)_s$ glass fibre-epoxy laminate fatigue loaded

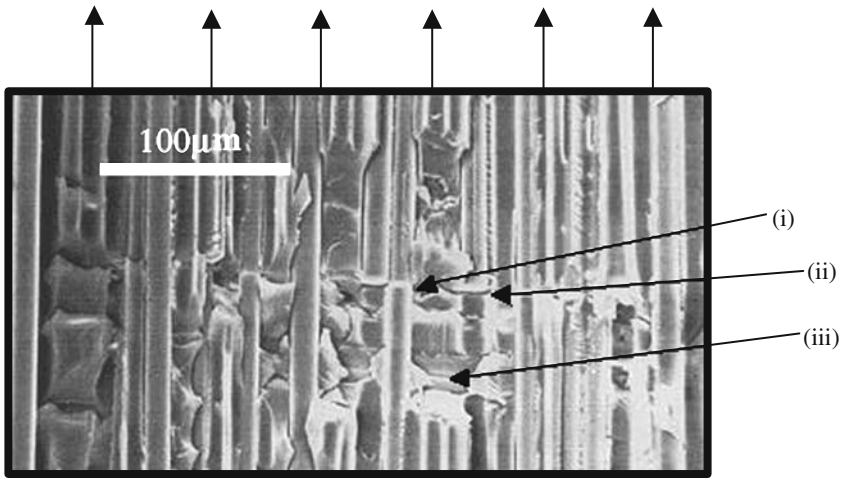

Fig. 7 De-lamination crack surface of a (0/90) interface in a $(0/90)_s$ glass fibre-epoxy laminate fatigue loaded. Revealed are (i) broken (0^o) fibres and (ii) a transverse ply crack; also, (iii) fibres are visible in the adjacent (90) ply

(As before, Eq. (7) is made dimensionless by normalising E_c with respect to the un-damaged modulus, E_o, of the laminate (Eq. 6).

Next, consider that the damage zone now has an ''effective'' matrix crack spacing $(s- \ell_d)$, where $2\ \ell_d$. is the total de-lamination crack length. Thus, when we substitute $(s- \ell_d.)$ into Eq. (5), we obtain for the modulus of that portion of (un-damaged) laminate (designated *(b)*):

$$\left[\frac{E_c}{E_0}\right]_b = \frac{1}{1 + \left(\frac{dE_2}{dE_1}\right)\frac{\tanh(\lambda(s-\ell_d))}{\lambda(s-\ell_d)}} \tag{8}$$

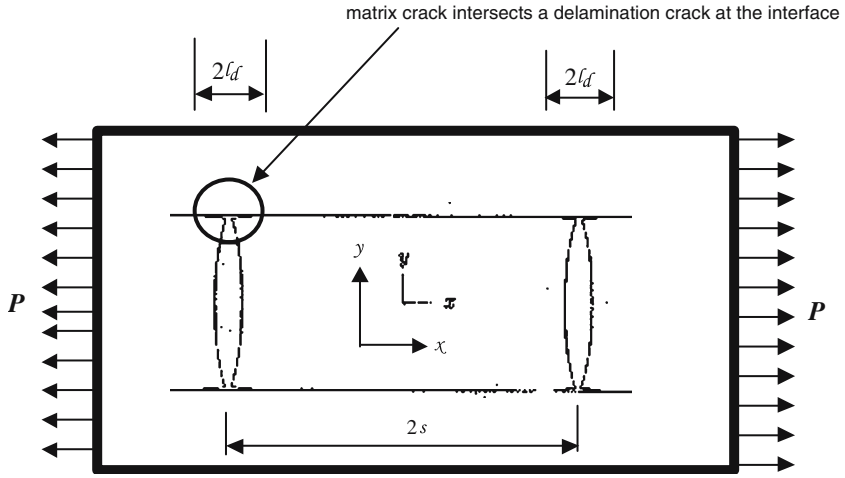

Fig. 8 This is an example of a physical model of coupled mechanisms. It is a model of a damaged $(0^o/90^o)_s$ cross-ply laminate under tensile load P (edge view). The geometry shows two neighbouring transverse ply cracks (of spacing $2s$) interacting with local de-lamination (inter-laminar) cracks of length $2\ell_d$

Finally, for a given applied tensile stress, the longitudinal modulus of the damaged laminate is calculated by using a rule of mixtures for $(E_c/E_o)_a$ and $(E_c/E_o)_b$:

$$\left[\frac{E_c}{E_0}\right]_{laminate} = \frac{\left[\frac{E_c}{E_0}\right]_a \left[\frac{E_c}{E_0}\right]_b (s)}{\left[\left[\frac{E_c}{E_0}\right]_b (s-\ell_d) + \left[\frac{E_c}{E_0}\right]_a (\ell_d)\right]} \tag{9}$$

Mapping stiffness change with damage accumulation

Consideration of transverse ply cracking only

Prediction of the reduced (or damage) modulus of the families of cross-ply glass fibre and carbon fibre-epoxy laminates, by considering the effect of matrix cracking only (Eq. 5), is shown in Figs. 9 and 10. The input to the model is the internal state variable D (= 1/s). Matrix crack spacing, s, is measured using in-situ dynamic SEM. These diagrams display sets of (normalised) modulus curves as a function of matrix crack spacing, s, (where s is normalised with respect to the transverse ply thickness, d). Thus, where d/s = 1, crack spacing is equivalent to ply thickness. As d/s tends to zero, the crack spacing tends to infinity and we arrive at the un-damaged material state (where E_c/E_o = 1).

Observe that the decrease in modulus with matrix cracking is greater for those laminates constructed from ''thicker'' (meaning multiple layered) transverse (90^o) plies, which we confirmed by experiment [14] and by finite element analysis [14]. The matrix crack density goes up, (i.e., D increases), with increasing load, (or load cycling), until the transverse ply becomes saturated with cracks; the (90^o) ply now becomes (more or less) load-free. At this

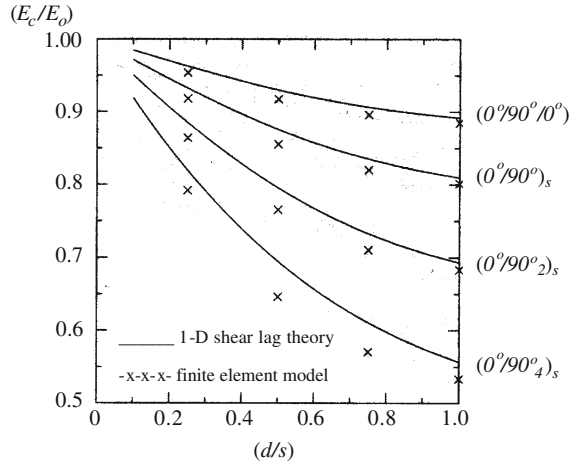

Fig. 9 Physical model of matrix cracking only compares favourably with the finite element result for the loss of stiffness of glass fibre-epoxy laminates with transverse ply cracking

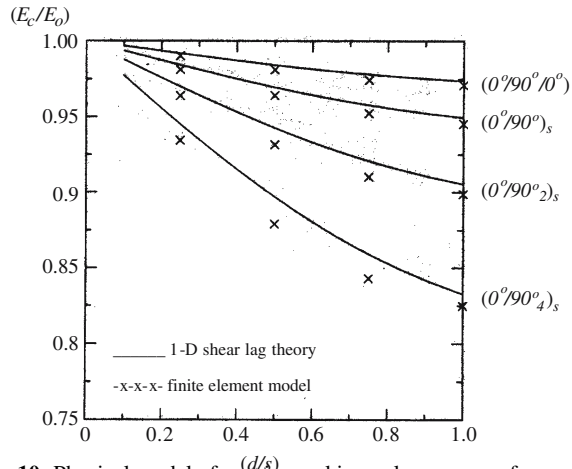

Fig. 10 Physical model of matrix cracking only compares favourably with the finite element result for the loss of stiffness of carbon fibre-epoxy laminates with transverse ply cracking

point, the modulus of the laminate approaches that value predicted by Eq. (7). Also, shown in these figures for comparative purposes, is the prediction of modulus based on a finite element analysis [14]. Agreement between the finite element model and the physical model is excellent, which supports our simple physical interpretation.

Coupling de-lamination cracking with matrix cracking

Adaptation of the transverse ply cracking (shear lag) model to include the effect of de-lamination cracking, (Eq. 9), is shown in Figs. 11 and 12. Here, contours of normalised (damage) modulus, E_c, as a function of (local) de-lamination crack length, ℓ_d, (normalised with respect to matrix crack spacing, s), are computed for a selected spacing of $s = 4d$.

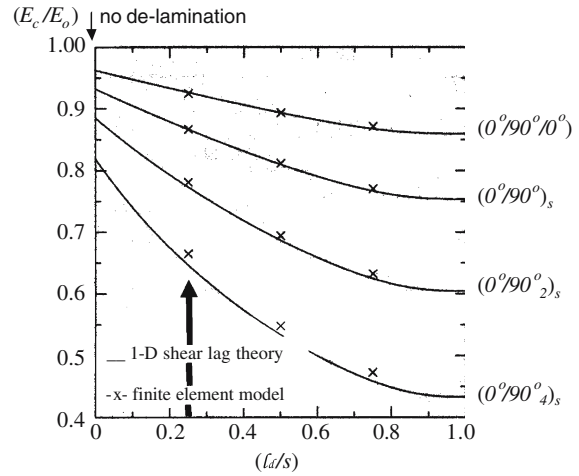

Fig. 11 Physical model of coupled matrix and de-lamination cracking compares favourably with the finite element result for the (damage) modulus of glass fibre-epoxy laminates

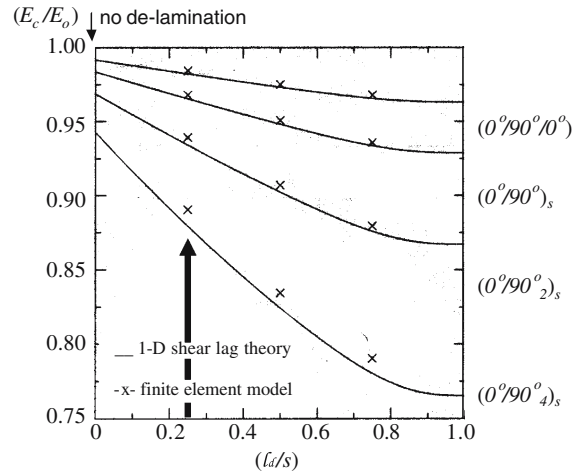

Fig. 12 Physical model of coupled matrix and de-lamination cracking compares favourably with the finite element result for the (damage) modulus of carbon fibre-epoxy laminates

In the absence of localised de-lamination cracking, the (damage) modulus is indicated on the left axis, which is equal to the reduced modulus indicated in the previous two figures, corresponding to where $d/s = 0.25$ on the horizontal axis (indicated by the arrow in Figs. 11, 12). Thus, the modulus of a laminate, in which the de-lamination crack has extended completely between two neighbouring matrix crack tips, is effectively equivalent to there being a multiplicity of closely-spaced matrix cracks. Now, the (damage) modulus is determined by the stiffness of the longitudinal ply only (Eq. 7).

In Figs. 13 and 14, contours of (normalised) modulus E_c as a function of (normalised) de-lamination crack length, ℓ_d, have been computed for selected values of s, equal to 1, 2, 4, and 8 times the transverse ply thickness, d.

From these figures, we see that, for the general family of $(0^o_i/90^o_j)_{ns}$, the (damage) modulus is a non-linear function of de-lamination crack length for all crack geometries. This is pronounced in laminates having ''thick'' transverse (90^o) plies, (meaning more than two plies, $j \geq 2$, i.e., for laminates of $(0^o/90^o_2)_s$ and $(0^o/90^o_4)_s$ configuration).

Finite element model of (damage) fracture stress

The finite element model of residual (post-fatigue) fracture stress of the laminate is based on the residual strength of the longitudinal (0^o) plies [14]. Inputs to the model include the elastic constants E_1, E_2, G_{12}, v_{12}, v_{21}, which can be determined by experiment. The length of the matrix crack is determined by thickness of the transverse (90^o) ply. Other structural variables include matrix crack spacing, s, and de-lamination crack length, ℓ_d. In-situ scanning electron microscopy (SEM) enabled us to measure the de-lamination crack size and crack spacing in monotonic and cyclic (fatigue) loading.

The three in-plane local stresses, σ_x, σ_y, and τ_{xy}, in the vicinity of a transverse ply matrix crack are shown in Fig. 15. It is the longitudinal stress, σ_x, which is responsible for matrix cracking and fibre fracture; the other two stresses combine to bring about de-cohesive failure of the ($0^o/90^o$) interface (de-lamination crack growth).

For a cross-ply laminate, the two plies of (0^o) and (90^o) are modelled as two perfectly elastic solids of different modulus and Poisson ratio, joined at a common surface (interface) (Fig. 16). Loading the cracked cross-ply laminate is simulated by applying a fixed displacement to one end of the specimen, constraining appropriate edges, while leaving a crack surface free. Meshes were constructed using 8-node quadrilateral plane-strain elements. An idealised mesh of our finite element model [14] of a coupled matrix crack and de-lamination crack is shown in Fig. 17.

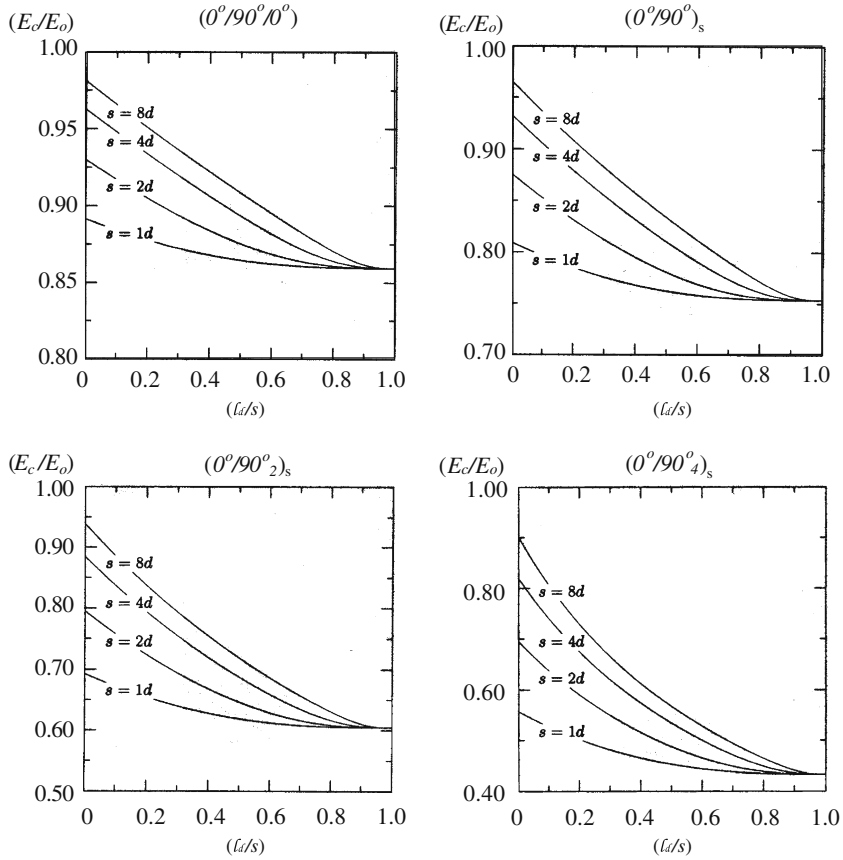

Fig. 13 Effect of local de-lamination cracking on the (damage) modulus of glass fibre-epoxy laminates having fixed distribution of cracks in the transverse ply

Crack tip damage zone: local tensile stress (σ_x) in the (0^o) ply of a (0^o/90^o/0^o) laminate

Under monotonic and cyclic tensile loading of a (0^o/90^o/0^o) glass fibre laminate, (close to ultimate fracture in both cases), the local stress, σ_x, in the longitudinal (0^o) ply in the vicinity of a matrix crack tip looks like this (Fig. 18). Whilst there is similarity between the pattern of stress (σ_x) field contours for both static and dynamic (cyclic) loading, the magnitude of σ_x is some 20–30% less in the fatigue-damaged material. Observe in the simple tensile test, (Fig. 18a), however, that the 1.2 GPa stress contour (arrowed) around the matrix crack tip encapsulates a volume of material equivalent to that of the 1 GPa stress contour (arrowed) of the fatigue-damaged specimen (Fig. 18b). Also note, that our experimental measurement of post-fatigue-strength is 20% lower than the specimen we tested in monotonic loading (see Table 1). We propose that in fatigue, there is greater damage originating from transverse ply (matrix) cracking, which includes a higher density of glass fibre fracture in the load-bearing (0^o) ply at the point of ultimate failure. Quite simply, the effect of cyclic loading is to further weaken the (0^o) ply, which results in a lower post-fatigue strength of the glass fibre-epoxy laminate than measured in a monotonic tensile test.

In the example of a (0^o/90^o/0^o) carbon fibre-epoxy laminate (Fig. 19), the pattern of localised stress (σ_x) field contours in the (0^o) ply is, more or less, identical to that of the equivalent glass fibre laminate (Fig. 18). However, closer inspection shows that the localised volume of (0^o) ply adjacent to the matrix crack tip, at the point of fast fracture, is smaller for the carbon fibre laminate. Increasing the number of (90^o) carbon fibre plies has little affect on the stress field pattern. Our proposal, which we build upon below, is this; it is the fracture of individual carbon fibres adjacent to one another, or clusters of fibre breaks within the matrix crack tip zone that produces a single ''large crack'' that subsequently propagates catastrophically. For glass fibre-epoxy, it is the volume of material within a matrix crack tip zone that affects the fracture stress by degrading the strength of the load bearing (0^o) plies; like other ceramic material systems, fracture stress is volume (size) dependent.

Crack tip damage zone: local tensile stress (σ_x) in the (0^o) ply of a (0^o/90^o_4)$_s$ laminate

In a cross ply laminate consisting of eight transverse plies, (90^o_4)$_s$, of glass fibre, at the point of ultimate tensile fracture, the local tensile stress of the (0^o) ply in the

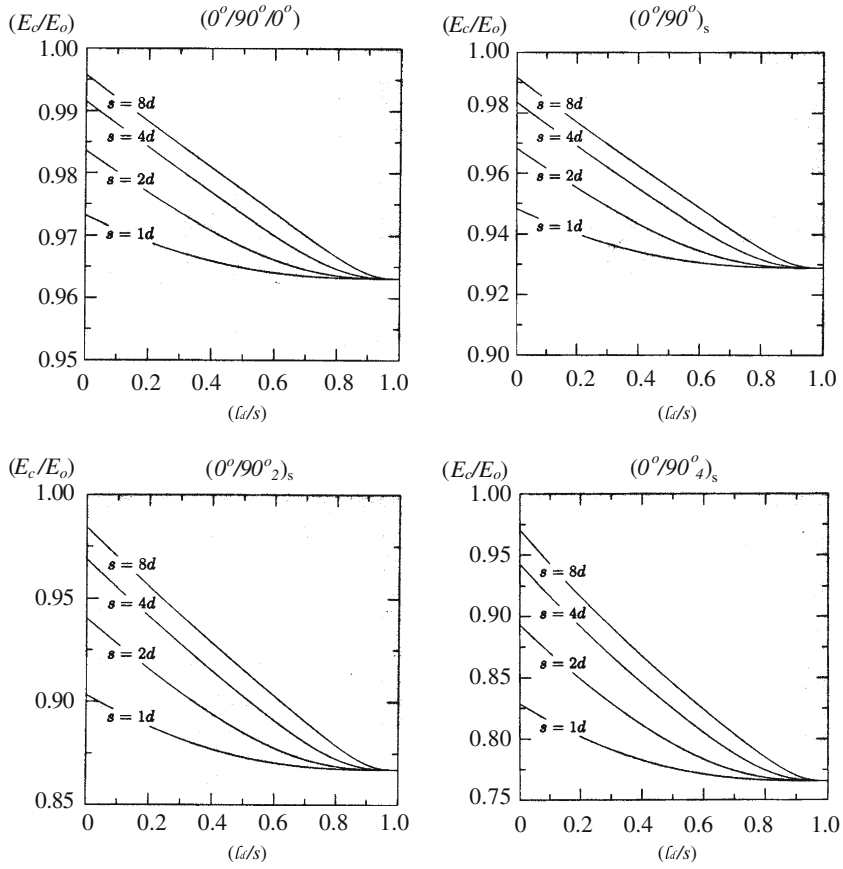

Fig. 14 Effect of local de-lamination cracking on the (damage) modulus of carbon fibre-epoxy laminates having fixed distribution of cracks in the transverse ply

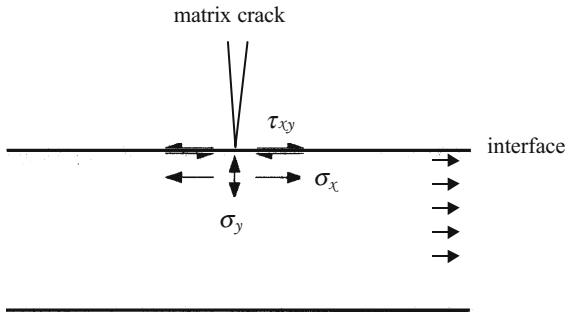

Fig. 15 Stress components at the tip of a transverse ply crack, which can lead to the formation of an interfacial crack (de-lamination crack) and/or longitudinal ply cracking and fracture

vicinity of the matrix and de-lamination crack tips, looks quite different than for the laminate containing a single (90^o) ply (Fig. 20). As before, however, when comparing the static picture with the dynamic one, we see a similarity between the two tensile stress contour maps. Looking no further than the simplest possible failure criterion, we propose that ultimate fracture occurs when the average localised tensile stress, σ_x, within a critical local volume of material attains some critical value; as before, strength depends on size.

Whilst this straightforward proposal may appear sound when applied to the laminate containing the single (90^o) ply, can it be applied successfully to explain the strength of the laminate containing eight $(90^o{}_4)_s$ plies? Observation of the stress field map clearly shows there is greater volume of the (0^o) ply under high tensile stress, (1 GPa, or so), in the vicinity of the matrix crack tip. We might, therefore, expect the strength of the laminate containing the eight $(90^o{}_4)_s$ plies to be less strong. By experiment, we confirmed that the strength of the laminate containing eight $(90^o{}_4)_s$ plies is 20% lower than that of the single (90^o) ply laminate construction (see Table 1). Thus, there is evidence to support the idea of a size (volume) dependence on strength.

Post-fatigue strength and internal structure of damaged laminates

Effect of transverse ply thickness on the fracture stress and ultimate failure strain

In a series of experiments on cross-ply laminates of variable transverse ply thickness, measurements were made of the ultimate tensile strength and ultimate failure strain of (at least) 30 identical tensile test coupons [14]. These ''dog-bone'' waisted specimens were either loaded to fracture in a monotonic tensile test or sacrificed in this

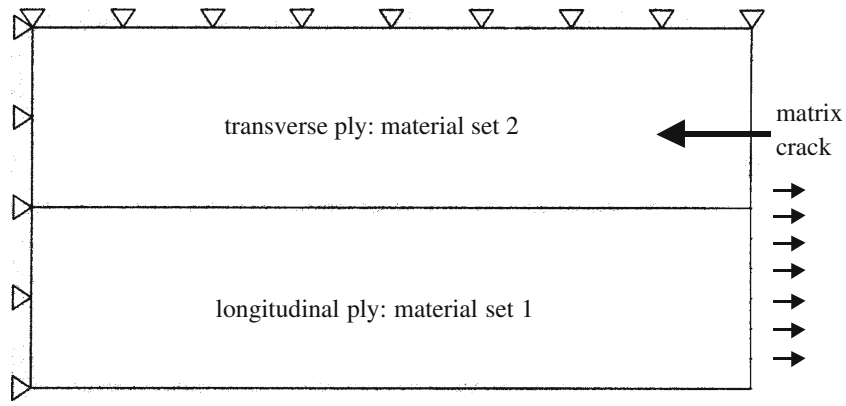

Fig. 16 Geometry of a cracked laminate used in the finite element model

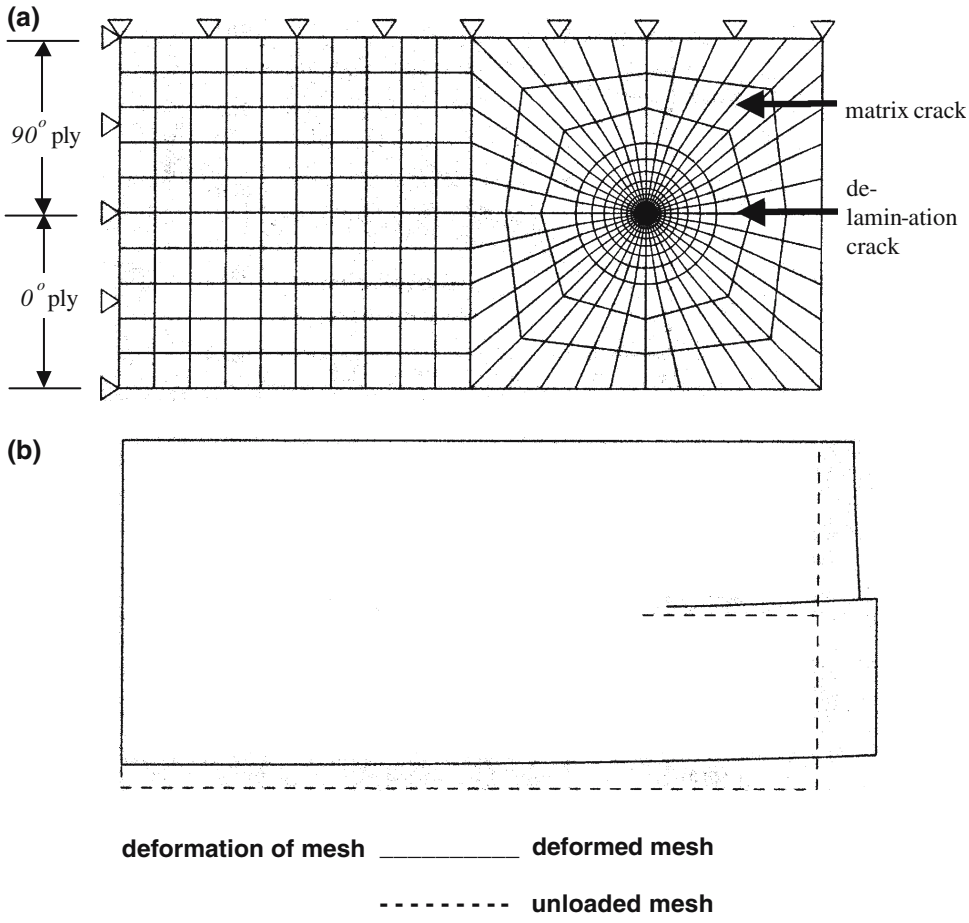

Fig. 17 Idealised meshing of $(0/90)_s$ laminate containing a transverse crack and de-lamination crack at its tip. The displaced profile of the loaded laminate shows contact elements preventing penetration of the crack surfaces

manner following tensile cyclic (fatigue) loading (at 5 Hz) for 3,000 or 10,000 cycles. For the glass fibre-epoxy laminate, specimens were fatigue loaded at a maximum tensile stress, σ_{max}, of 600 MPa, (where $\sigma_{max} = 0.5$ ultimate strength, with a load ratio $R = 0.2$). In the case of carbon fibre-epoxy laminates, the maximum tensile stress in the fatigue cycle was 720 MPa (or 35% ultimate strength). The fracture stress data were plotted on Weibull graph paper (Fig. 21) and the Weibull coefficients, including the average fracture stress, were determined accordingly. A typical set of data for $(0/90)_s$ glass fibre-epoxy laminates is shown in Table 1.

Note that these stresses have been calculated on the premise that only the (0^o) plies are carrying substantial load. In this way, failure stresses of laminates in a given family can be compared directly in a straightforward manner. This is reasonable because at ultimate failure, the transverse ply has become saturated with matrix cracks and is essentially non-load carrying, with maximum load having been transferred on to the longitudinal plies.

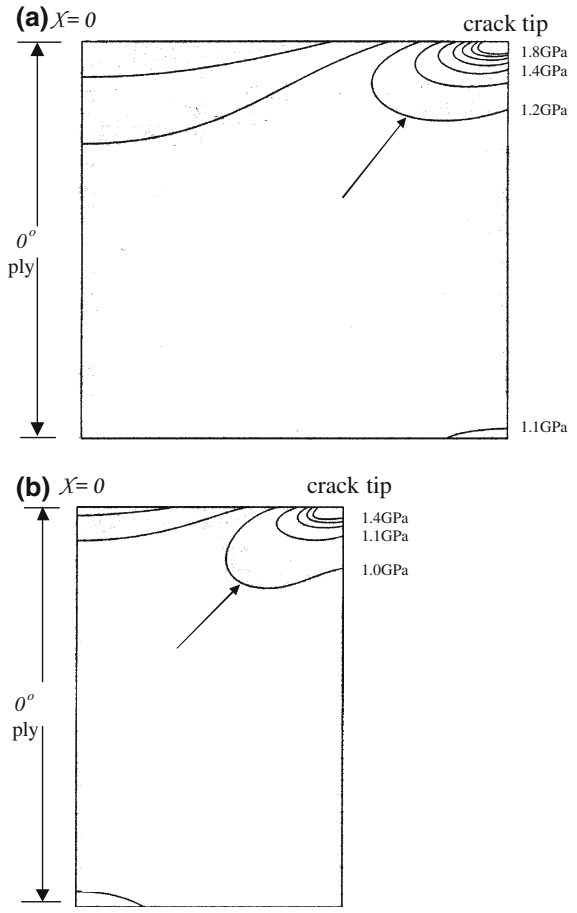

Fig. 18 (**a**) Distribution of tensile stresses in the longitudinal (0^o) ply of a ($0^o/90^o/0^o$) glass fibre-epoxy laminate at the point of fast fracture. Static failure geometry: s = 0.16 mm, σ_{max} = 8.58 GPa, σ_f = 1.24 GPa (**b**) Distribution of tensile stresses in the longitudinal (0^o) ply of a ($0^o/90^o/0^o$) glass fibre-epoxy laminate at the point of fast fracture of the fatigue-damaged specimen. Post-fatigue failure geometry: s = 0.10 mm, σ_{max} = 6.34 GPa, σ_f = 1.04 GPa

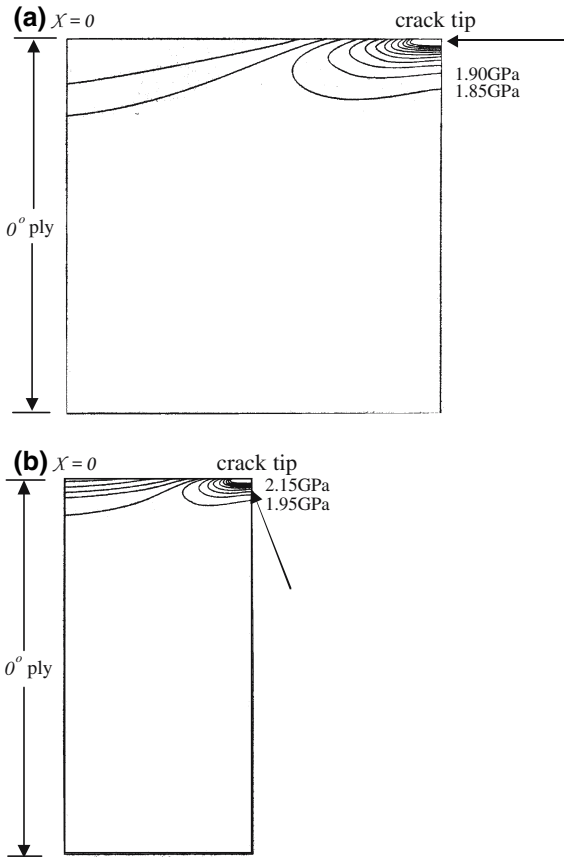

Fig. 19 (**a**) Distribution of tensile stresses in the longitudinal (0^o) ply of a ($0^o/90^o/0^o$) carbon fibre-epoxy laminate at the point of fast fracture. Static failure geometry: s = 2d, σ_{max} = 11.9 GPa, σ_f = 1.91 GPa. (**b**) Distribution of tensile stresses in the longitudinal (0^o) ply of a ($0^o/90^o/0^o$) carbon fibre-epoxy laminate at the point of fast fracture. Post-fatigue failure geometry: s = d, σ_{max} = 11.1 GPa, σ_f = 2.02 GPa

Roughly speaking, the Weibull modulus (m) for the entire family of carbon fibre laminates (m = 20) is twice that of the glass fibre laminates (m = 12), irrespective of lay-up geometry. On the other hand, the Weibull (reference) stress, σ_o, (or mean (or average)) tensile strength, σ_u, and post-fatigue tensile strength, σ_f, of the two composite systems, does depend upon transverse ply thickness. These trends in the ultimate tensile strength and post-fatigue strength with transverse ply thickness and number of fatigue cycles is examined below in terms of a strain to failure criterion.

Glass fibre-epoxy laminates $(0^o_i/90^o_j)_s$

The effect of transverse ply thickness, (where j = 1, 2, 4), on the ultimate tensile strength and post-fatigue (residual) strength of the longitudinal ply (0^o_i), (where i = 1), is summarised in Fig. 22. The two curves showing the monotonic tensile strength and post-fatigue strength after 10,000 load cycles have been drawn through the experimental values of mean (average) fracture stress obtained in the Weibull tests. For the sake of clarity, the actual spread of data points (30 points per lay-up) have been omitted. The standard deviation is of the order of 0.1 GPa for both sets of data.

Based on experimental evidence and observation, we propose:

(1) where $j \geq 2$, fatigue induces appreciable matrix cracking and de-lamination, and there is no significant differences between the monotonic tensile strength and post-fatigue fracture stress;
(2) where $j \leq 2$, load cycling (10,000 cycles) induces sufficient fibre breakage to reduce the strength rapidly below that of the tensile strength measured in a simple monotonic tensile test.

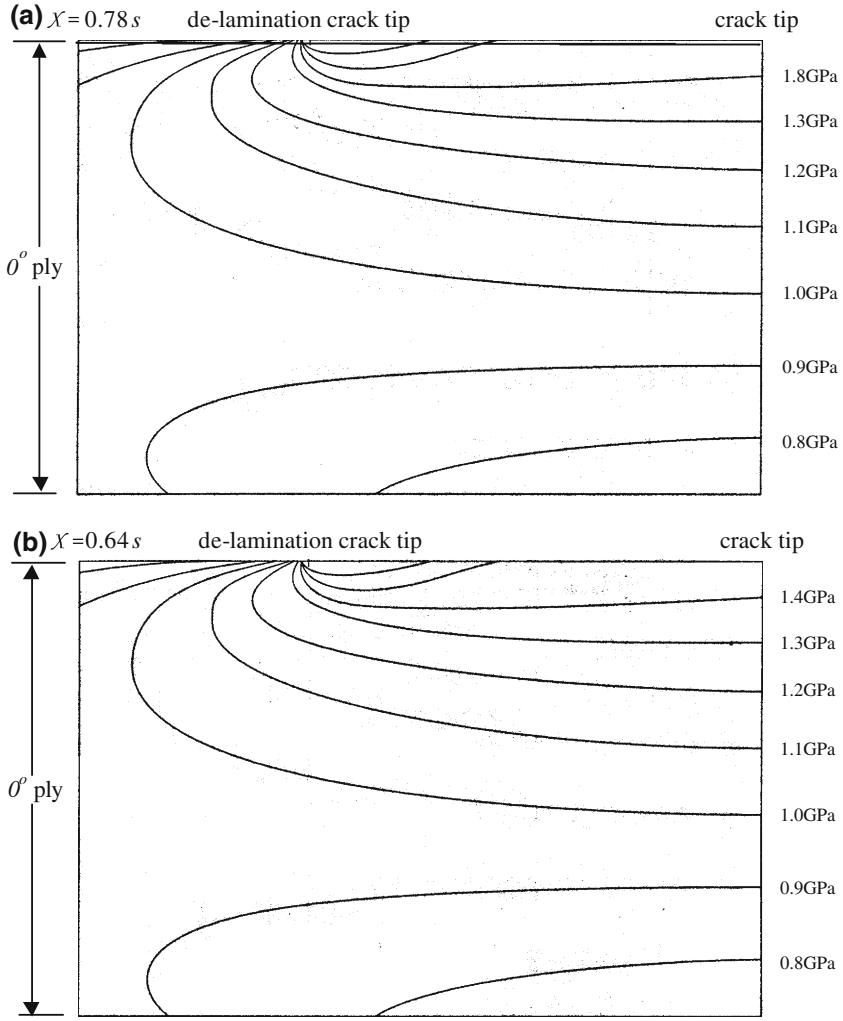

Fig. 20 (**a**) Distribution of tensile stresses in the longitudinal (0^o) ply of a $(0^o/90^o_4)_s$ glass fibre-epoxy laminate at the point of fast fracture. Static failure geometry: s = 1.0 mm, σ_{max} = 5.16 GPa, σ_f = 1.06 GPa. (**b**) Distribution of tensile stresses in the longitudinal (0^o) ply of a $(0^o/90^o_4)_s$ glass fibre-epoxy laminate at the point of fast fracture. Post-fatigue failure geometry: s = 0.62 mm, σ_{max} = 4.85 GPa, σ_f = 1.1 GPa

Table 1 Weibull coefficients, (σ_o) and (m), and average strength (σ_{av}) of glass fibre-epoxy and carbon fibre-epoxy cross-ply laminates

Laminate geometry	Glass fibre-epoxy (0/90/0)	Glass fibre-epoxy $(0/90)_s$	Glass fibre-epoxy $(0/90_2)_s$	Glass fibre-epoxy $(0/90_4)_s$
Reference stress (σ_o) (GPa)	1.293	1.242	1.183	1.114
Weibull modulus (m)	12.4	14.7	9.51	10.44
Av. tensile strength (σ_{av}) (GPa)	1.243	1.201	1.125	1.064
After 3,000 load cycles (σ_o) (GPa)	1.153	1.158	1.154	1.138
After 3,000 load cycles (m)	12.0	9.3	13.9	11.4
Av. tensile strength (σ_{av}) (GPa)	1.107	1.101	1.114	1.091
After 10,000 load cycles (σ_o) (GPa)	1.098	1.161	1.21	1.162
After 10,000 load cycles (m)	8.9	15.3	11.0	8.1
Av. tensile strength (σ_{av}) (GPa)	1.040	1.124	1.153	1.096
Laminate geometry	Carbon fibre-epoxy (0/90/0)	Carbon fibre-epoxy $(0/90)_s$	Carbon fibre-epoxy $(0/90_2)_s$	Carbon fibre-epoxy $(0/90_4)_s$
Reference stress (σ_o) (GPa)	1.952	1.954	2.220	2.377
Weibull modulus (m)	21.5	22.5	14.9	15.4
Av. tensile strength (σ_{av})(GPa)	1.906	1.910	2.147	2.302

The transition between there being a fatigue effect on residual (damage) tensile strength and there not being one, takes place where the transverse ply thickness is about 0.45 mm (or $3d$). In fatigue, we observed progressive fibre fracture in laminates (where $j \leq 2$) with increasing number of load cycles. In identical material subjected to a monotonic tensile test, fibre fracture was observed only at the point of fast facture. Where $j \geq 2$, de-lamination cracking

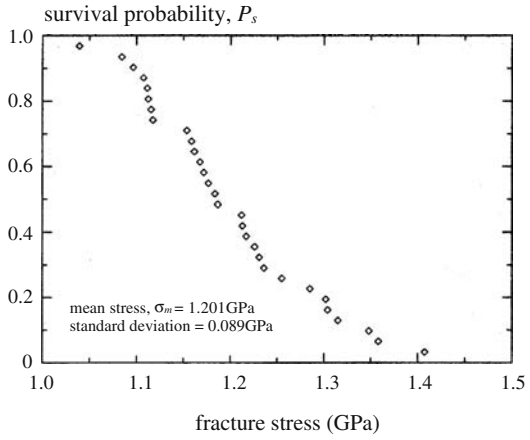

Fig. 21 Fracture stress distribution (survival probability) of $(0/90)_s$ glass fibre-epoxy laminates

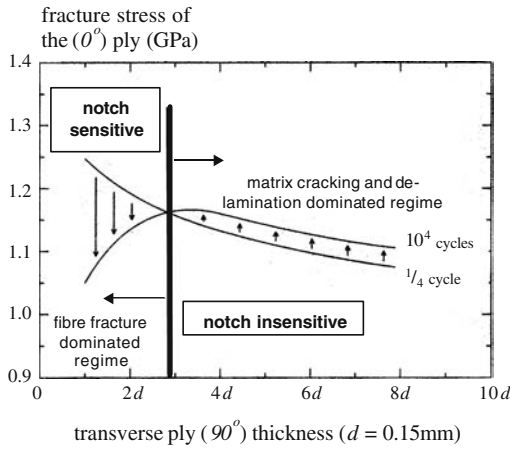

Fig. 22 Effect of transverse ply thickness on the tensile strength and residual strength of fatigue-damaged glass fibre-epoxy laminates

at transverse ply matrix cracks dominates the total failure process. We conclude that the absence (or lack) of de-lamination cracking at the $(0^o/90^o_j)$ interface (where $j \leq 2$) renders the material notch sensitive (Fig. 22).

In constant stress amplitude cycling of laminates containing four transverse (90^o) plies ($j \geq 2$), we observed the density of matrix cracks to increase with number of cycles; crack spacing, s, shortens (see Table 2). In essence, the material ''work softens'' and becomes more compliant (stiffness or modulus falls). The result is that the strain to failure of the laminate increases with the accumulation of fatigue damage. On the other hand, where thickness of the (90^o) ply is less than $4d$, ($j \leq 2$), we found the reverse to be true; i.e., the post-fatigue strain to failure was less than that measured in a simple tensile test. We postulate that in the vicinity of closely spaced matrix crack tips, glass fibres in

Table 2 First ply cracking stress (strain), crack opening and crack spacing in monotonic and cyclic (fatigue) loading for glass fibre-epoxy

	(0/90/0)	$(0/90)_s$	$(0/90_2)_s$	$(0/90_4)_s$
First ply cracking stress* (GPa)	1.06	0.86	0.72	0.67
First ply cracking strain (%)	2.42	1.79	1.16	0.76
Crack opening (μm) (at first ply cracking)	3	5	11	25
Ultimate fracture stress (GPa)	1.24	1.20	1.12	1.06
Crack opening (μm) (at ultimate failure)	5	9	15	30
Crack spacing (μm) ($^1/_4$ cycle)	160	250	500	1000
Crack spacing (μm) (10,000 cycles)	100	180	340	620

Measurements were made on tensile specimens under load in the SEM

*All stresses are expressed as (0^o) ply stresses

the (0^o) ply fracture in fatigue, which weakens the material below its monotonic tensile strength. In our in-situ SEM study of the fatigue failure of $(0^o/90^o/0^o)$ and $(0^o/90^o)_s$ laminates, we observe clearly a concentration of broken glass fibre within (0^o) longitudinal plies in front of matrix crack tips.

Carbon fibre-epoxy laminates $(0^o_i/90^o_j)_s$

The effect of transverse ply thickness, (where j = 1, 2, 4), on the monotonic tensile strength and post-fatigue (residual) strength of the longitudinal ply (0^o_i), (where i = 1), is summarised in Fig. 23.

To begin with, note that where $j \leq 2$, in monotonic loading the laminate is weaker than material that has been fatigue loaded. This observation is in contrast to our experimental result for the glass fibre composite depicted in Fig. 22. Furthermore, where $j \geq 2$, fatigue cycling degrades residual strength. This, too, contrasts with the behaviour of the glass fibre laminate. Whilst matrix cracks do form in the transverse ply, which renders the carbon fibre laminate more compliant (stiffness falls), the mechanism of fibre fracture is a difficult one to quantify. Our knowledge of the fatigue damage state based on fracture of carbon fibres and de-lamination is lacking in detail.

Nonetheless, we attempted a delicate procedure to investigate the fracture of carbon fibre [34] by de-plying (at 400 °C or thereabouts) the mechanically damaged laminate, and scanning in the SEM the surface of the separated longitudinal ply, looking for and counting fibre breaks (see below). Unless the longitudinal ply is susceptible to fibre fracture in cyclic loading, we might expect the post-fatigue (residual) strength to be affected little. The fatigue data displayed in Fig. 23 would support the hypothesis that the strength of the (0^o) ply is essentially insensitive to transverse ply thickness over this range, more

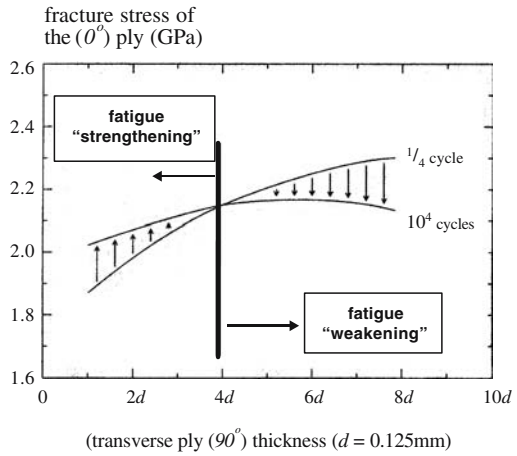

Fig. 23 Effect of transverse ply thickness on the strength of fatigue-damaged carbon fibre-epoxy laminates

or less, and is affected little by load cycling up to 10,000 cycles.

A failure strain criterion of post-fatigue strength

If a laminate suffers no loss in strength with load cycling but the modulus, E_c, falls with damage accumulation, for small displacements we can determine the post-fatigue strain to failure using Hooke's law (Eq. 10). From a knowledge of matrix crack spacing and de-lamination crack length gained from our in-situ SEM work, thereby inserting such values of s and ℓ_d into Eq. (9), would enable us to predict the reduced (damage) modulus, E_c of the laminate.

Consider a simple tensile test, (or constant cyclic maximum stress) for small elastic displacement of the laminate, the relation between ultimate tensile strength, σ_f, and ultimate failure strain, ϵ_f, is given simply by:

$$\varepsilon_f = \frac{\sigma_f}{E_c} \tag{10}$$

(where E_c is the Young's modulus). Now re-call Eq. (9) for the reduced (damage) modulus E_c of a laminate:

$$\left[\frac{E_c}{E_0}\right]_{\text{lam}} = \frac{\left[\frac{E_c}{E_0}\right]_a \left[\frac{E_c}{E_0}\right]_b (s)}{\left[\left[\frac{E_c}{E_0}\right]_a (s-\ell_d) + \left[\frac{E_c}{E_0}\right]_a (\ell_d)\right]}$$

Whilst fibre fracture in the (0^o) ply would undoubtedly influence the fracture stress of the laminate, it would be prudent to refrain from hazarding a guess as to its effect on tensile modulus. Thus, if for the time being we ignore any possible effect of broken fibres on the modulus, then by estimating the reduced (damage) modulus due to matrix and de-lamination cracking using Eq. (9), and substituting for E_c into Eq. (10), we can predict the ultimate failure strain (Table 3) and compare with experimental measurement. Inputs to the model (Eq. 9) are the experimental (in-situ SEM) values of matrix crack spacing, s, and de-lamination crack length, ℓ_d. (For the carbon fibre-epoxy laminate we approximated $s = 2d$ for static loading and $s = d$ for cyclic loading).

Table 3 Ultimate tensile failure strain ϵ_f (%) of the laminate predicted by combining equations (9, 10) together with experimental measurements of matrix crack spacing and de-lamination crack length made on tensile specimens under load in the SEM

Static or cyclic loading	Laminate configuration	Glass fibre-epoxy (%ϵ_f)	Carbon fibre-epoxy (%ϵ_f)
Static	(0/90/0)	2.95	1.38
Static	$(0/90)_s$	2.72	1.36
Static	$(0/90_2)_s$	2.27	1.45
Static	$(0/90_4)_s$	1.88	1.46
Cyclic	(0/90/0)	2.55	1.48
Cyclic	$(0/90)_s$	2.65	1.51
Cyclic	$(0/90_2)_s$	2.52	1.53
Cyclic	$(0/90_4)_s$	2.33	1.48

From the results in Table 3, we conclude that increasing the thickness (number) of transverse (90^o) plies reduces the monotonic tensile failure strain, ϵ_f, of the glass fibre-epoxy laminate. Closer inspection shows that in cyclic loading, the strain to failure, ϵ_f, of glass fibre-epoxy laminates containing only one or two transverse plies decreases, whilst ϵ_f for the composite containing four and eight transverse plies increases. For comparison, however, the failure strain of carbon fibre-epoxy laminates is independent of transverse ply thickness ($\epsilon_f \sim 1.4$–1.5%).

We know that fatigue-damaged material is more compliant, (its crack density is greater than from monotonic loading), and, therefore, according to Eq. (10) ϵ_f would be expected to increase. Such logic seems to be valid, however, only for the fatigue-damaged glass fibre laminate containing the thicker (four or more) transverse plies. One possible explanation that is physically sound is to propose that significant fibre fracture has occurred in the (0^o) ply adjacent to the thinner (less than four) transverse plies. The consequence of this would be to simultaneously reduce the ultimate fracture stress and ultimate failure strain of the laminate.

Now since the strain to failure of the complete family of carbon fibre cross-ply laminates is relatively constant, perhaps a slight increase in ϵ_f with cyclic loading, we

would have to argue in favour of little or no significant (meaning not detrimental) fibre breakage during fatigue prior to ultimate failure. In which case, any slight increase in strain to failure with cyclic loading would be due to some additional matrix cracking.

Some evidence of fracture of carbon fibres in fatigue of $(0^o/90^o)_s$

In some carefully performed fatigue experiments on the carbon fibre laminates, the progressive nature of the fracture of individual carbon fibre was investigated by examining in the SEM the de-laminated surface of a longitudinal (0^o) ply removed from a de-plied $(0^o/90^o)_s$ carbon fibre laminate [34]. This involved sacrificing a large number of low cycle fatigue specimens at intervals of 1,000 load cycles to begin with, followed by sacrificing specimens at intervals of 10,000 cycles as high cycle fatigue damage accumulated. In this procedure, the stage of the SEM was carefully manipulated back and forth over the surface area of the de-plied longitudinal ply, scanning over a total surface area of 4 mm by 3 mm, counting broken carbon fibres in the process. The mapping of fibre breaks was carried out in the proximity of closely spaced transverse ply matrix crack tips. This delicate technique, developed by my graduate student, Dr Moses Otunga, was used extensively in his graduate research at Cambridge [34].

In essence, a grid of 1 mm squares, made of 0.1 mm wide aluminium, was positioned over the surface of the de-plied (0^o) ply in the vicinity of transverse ply cracks and the sample systematically scanned in the SEM. The results are presented below as the density of broken fibres per mm^2 plotted against load cycles for different maximum stress in the cycle (Figs. 24, 25). As a first approximation, after 10^6 load cycles, the density of fibre breaks ranges

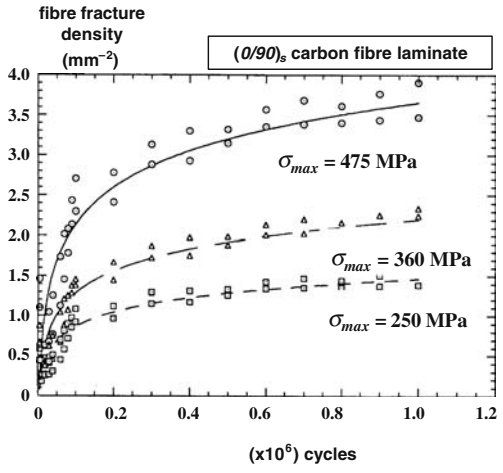

Fig. 24 Fibre fracture accumulation with fatigue damage

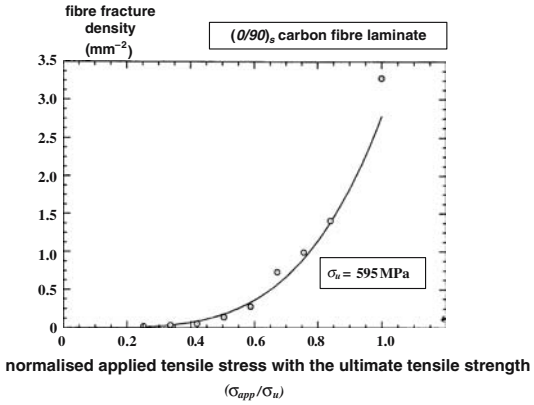

Fig. 25 Fibre fracture density under monotonic loading

between 1 and 4 fibres for every square millimetre of surface area of de-plied (0^o) layer scanned, depending on the maximum stress in the cycle (Fig. 24). If the thickness of a single (0^o) ply is equivalent to 15 fibre diameters deep (see Fig. 4), then the number of broken fibres in a cubic millimetre (mm^3) of that single (0^o) ply would be of the order of 15 times that observed on the surface. In other words, the fibre fracture density (number of broken fibres/mm^3) would now be as high as 50–60/mm^3 after 10^6 cycles at a cyclic maximum stress of 80% ultimate tensile strength. Most of these carbon fibres fracture in low cycle fatigue, 10^4cycles or less. At fracture in a monotonic tensile test, the maximum density of fibre breaks is also about 50/mm^3 with significant fibre fracture occurring predominantly above 60% ultimate strength.

When carbon fibres do fracture, they do so close to or in front of the tip of a transverse ply (matrix) crack. We have no evidence to indicate that the number of fibre breaks continues to increase beyond 10^6 cycles, although there must be a cascade of fibres snapping as the fatigue life-time of the specimen finally arrives. These estimated figures of fibre fracture density are based on the assumption that fibres break uniformly through the thickness of the (0^o) ply. This may not be the case. Reifsnider and Jamison reported that fibre fracture density decreases rapidly over a distance of only one or two fibres deep from the ($0^o/90^o$) interface [35, 36].

Summary and final remarks

The economic advantage of reducing the high cost of vast experimental programs in assorted environments and stress-states having duration of many thousands of hours is potentially huge. There is scope to integrate a physical modelling approach with the large experimental programmes that are currently employed to design fracture

critical components and structures. Added benefits include more options being made available to the designer, a reduced need for extensive and costly testing and more efficient and shorter design iteration cycles. This last point requires elaboration. Modelling a particular problem is only a sub-element of the overall design process. We believe that the philosophy behind the physical modelling approach has general applicability. In particular, the foundation of physical modelling could be applied to solving a range of problems in composites. Existing design methodologies at the higher structural size scales can be supported and justified by fundamental understanding at lower size scales.

Successful modelling of physical processes can be achieved by following a set of steps: identify the physical mechanisms (preferably by direct observation); construct the model (using previously modelled problems or applying existing modelling tools); test the model (by comparing with data) and tune the model (lumping together empirical parameters). In other words, determine the dominant mechanisms; simplify it (them); and exploit the modelling successes of others in materials science and engineering. Even now the job is still incomplete; the last word is *iterate*.

Acknowledgements Our work on the physical modelling of damage in composite materials has benefited from many valuable discussions with Professor Mike F Ashby, Cambridge University Engineering Department, and Professor Paul A Smith of the University of Surrey on this work in particular. RD was supported by a research grant from the Engineering and Physical Sciences Research Council.

References

1. Kedward KT, Beaumont PWR (1992) Intl J Fatigue 14(5):283
2. Spearing SM, Beaumont PWR (1998) Appl Compos Mater 5(2):69
3. Spearing SM, Lagace PA, McManus HLN (1998) Appl Compos Mater 5(3):139
4. Wells JK, Beaumont PWR (1981) In: Daniel IM (ed) ASTM STP 787 composite materials: testing and design (6th Conference) Phoenix, USA (12, 13 May), pp 147–162
5. Wells JK, Beaumont PWR (1982) Scr Metallurgica 16:99
6. Wells JK, Beaumont PWR (1985) J Mater Sci 20: 1275
7. Wells JK, Beaumont PWR (1985) J Mater Sci 20:2735
8. Wells JK, Beaumont PWR (1987) J Mater Sci 22:1457
9. Hogg PJ, Hull D (1980) Met Sci 14:441
10. Price JN, Hull D (1983) J Mater Sci. 18:2798
11. Price JN, Hull D (1987) Compos Sci Tech 28:193
12. Sekine H, Hu N, Fukunagah H (1995) Compos Sci Tech 53:317
13. Sekine H, Beaumont PWR (1998) Compos Sci Tech 58(10):1659
14. Dimant RA (1994) Damage mechanics of composite laminates. Cambridge University Engineering Department PhD Thesis
15. Dimant R, Shercliff H, Beaumont PWR (2002) Compos Sci Tech 62:255
16. Poursartip AP, Ashby MF, Beaumont PWR (1984) In: Ashbee KHG (ed) The fatigue damage mechanics of fibrous composites, Polymer NDE, Terma do Vimeiro, Portugal (4–5th September). Technomic Publishers, Basel, Switzerland pp 250–260
17. Poursartip AP, Ashby MF, Beaumont PWR (1982) Scr Metallurgica 16:601
18. Poursartip AP, Ashby MF, Beaumont PWR (1986) Compos Sci Tech 25:193
19. Poursartip AP, Beaumont PWR (1986) Compos Sci Tech 25:283
20. Kortschot MT, Beaumont PWR (1990) Compos Sci Tech 39:289
21. Kortschot MT, Beaumont PWR (1990) Compos Sci Tech 39:303
22. Kortschot MT, Beaumont PWR, Ashby MF (1991) Compos Sci Tech 40:147
23. Kortschot MT, Beaumont PWR, (1991) Compos Sci Tech 40:167
24. Kortschot MT, Beaumont PWR (1993) Damage-based notched strength modeling: a summary. In: O'Brien TK (ed) Composite Materials: Fatigue and Fracture, ASTM STP 1110:55
25. Spearing SM, Beaumont PWR, Ashby MF (1991) Fatigue damage mechanics of notched graphite-epoxy laminates. In: O'Brien TK (ed) Composite Materials: Fatigue and Fracture, ASTM STP 1110:596
26. Spearing SM, Beaumont PWR (1992) Compos Sci Tech 44:159
27. Spearing SM, Beaumont PWR, ASHBY MF (1992) Compos Sci Tech 44:169
28. Spearing SM, Beaumont PWR (1992) Compos Sci Tech 44:299
29. Spearing SM, Beaumont PWR, Smith PA (1992) Compos Sci Tech 44:309
30. Spearing SM, Beaumont PWR, Kortschot MT (1992) Composites 23:305
31. Cowley KD, Beaumont PWR (1997) Compos Sci Tech 52:295
32. Cowley KD, Beaumont PWR (1997) Compos Sci Tech 52:310
33. Cowley KD, Beaumont PWR (1997) Compos Sci Tech 52:325
34. Cowley KD, Beaumont PWR (1997) Compos Sci Tech 52:334
35. Otunga M (1995) Fatigue damage accumulation in carbon fibre laminates. PhD Thesis, Engineering Department, Cambridge University
36. Reifsnider KL, Jamison RD (1982) Int J Fatigue 4:187
37. Jamison RD (1986) ASTM STP 907:252